Effect of anodizing voltage and pore widening time on the effective refractive index of anodic titanium oxide

N. A. Sapoletova[1], S. E. Kushnir[1,2]*, K. S. Napolskii[1,2]

[1]Department of Chemistry, Lomonosov Moscow State University, 119991, Moscow, Russia
[2]Department of Materials Science, Lomonosov Moscow State University, 119991, Moscow, Russia

*kushnir@elch.chem.msu.ru

The unique optical properties of porous anodic titanium oxide (ATO) make it a promising material for solar energy conversion, sensorics, and opto-electronics. The optical path length and effective refractive index (n_{eff}) of ATO can be tuned by chemical etching of pore walls. However, precise control of these optical parameters is still challenging due to the lack of data on the effect of pore widening time on the n_{eff}. Here, a detailed study of the influence of anodizing voltage and pore widening time on the n_{eff} of the ATO films was performed. Analysis of reflectance spectra of ATO synthesized at 35 – 50 V shows that pore widening in 3 wt. % H_2O_2 aqueous solution allows one to control the n_{eff} at values ranging from 1.54 to 1.84. The data required for the prediction of the thickness, n_{eff}, and optical path length of the ATO films from anodizing and etching conditions are obtained.

Keywords: anodic titanium oxide, anodization, porous materials, film, refractive index, optical materials and properties.

Received: 5 April 2019

Revised: 15 April 2019

1. Introduction

Anodizing is one of the more promising methods for the production of porous TiO_2 films at room temperature [1]. Porous anodic titanium oxide (ATO) films demonstrate high efficiency in water photoelectrolysis [2], photocatalysis [3, 4], gas sensing [5], and can be used as carriers for controlled drug release [6–8]. In addition, ATO films have potential for application in dye-sensitized solar cells [9], refractive index sensors [10, 11], smart color windows, and electronic displays [12] owing to a high refractive index ($n_{TiO_2} = 2.6$ at $\lambda = 600$ nm [13]) and semiconductor properties of titanium oxide.

Optical path length of ATO films, the product of the film thickness and refractive index, is one of the key parameters that has great importance for optical applications. The thickness of ATO is directly proportional to charge density consumed during anodizing [14, 15], whereas control of the refractive index of ATO more challenging. Taking into account a small diameter of the pores in ATO films, which is much lower than the wavelength of visible light, the effective refractive index (n_{eff}) of ATO is a function of film porosity within a framework of the effective medium model. It is worth noting that the porosity and the n_{eff} values for anodic oxides change during the anodizing process due to chemical etching of the pore walls [16]. To the best of our knowledge, there are no systematic data on the n_{eff} of ATO as a function of anodizing voltage and the duration of chemical etching.

Here, we study the dependence of the thickness-to-charge density ratio and the n_{eff} of ATO films on anodizing voltage. Special attention is paid to the variation of the n_{eff} caused by chemical etching of pore walls in the anodizing electrolyte and aqueous H_2O_2 solution.

2. Materials and methods

Prior to anodizing, titanium foils (0.15 mm thick, 99.6 % purity) were electrochemically polished in a mixture of 99.5 wt. % acetic acid and 65 wt. % perchloric acid with a volume ratio of 9:1. Electrochemical polishing was performed over 4 min under square-wave applied voltage (40 V for 10 s and 60 V for 10 s) at a temperature below 25 °C as described elsewhere [15].

To prepare porous anodic titanium oxide films, Ti was anodized at a constant voltage between 30 – 60 V in an ethylene glycol electrolyte containing 0.3 wt. % NH_4F, 0.66 wt. % CH_3COONa, and 2 wt. % H_2O at 30 °C. The electrolyte solution was prepared by adding aqueous NH_4F to sodium acetate dissolved in ethylene glycol. The electrolyte was stirred at 480 RPM using an overhead stirrer. Experiments were performed in a two-electrode electrochemical cell with the distance of 2 cm between Ti electrodes. The anodized area and the total charge density consumed during anodizing of each sample was 1.13 cm^2 and 3.36 C·cm^{-2}, respectively. To study pore

widening effect on the n_{eff} of the ATO in electrolyte, some of the prepared films were stored in electrolyte solution for 2 – 6 hours after anodizing. Finally, the ATO films were washed with ethanol and then air-dried. Some as-synthesized ATO films were aged in 3 wt. % H_2O_2 aqueous solution for 7.5 – 30 minutes under stirring.

Morphological characterization of the ATO films was performed by scanning electron microscopy (SEM) using LEO Supra 50 VP instrument. Perkin Elmer Lambda 950 spectrophotometer was used to record the reflectance spectra at incident angles of 8, 30, 45, 60, and 65° in a wavelength range of 650 – 890 nm.

3. Results and discussion

Optical reflectance spectra of the ATO films prepared at different anodizing voltages (U) are shown in Fig. 1a. In the case of the ATO obtained at $U = 35 – 50$ V, intense Fabry–Pérot oscillations of the reflectivity can be clearly seen in the spectra, resulting in high thickness uniformity for these samples at least across the irradiated area (4×4 mm^2). The Fabry–Pérot oscillations in the spectra of the samples, prepared at anodizing voltages outside the 35 – 50 V range, are weak or completely lacking, manifesting non-uniform thickness. Thus, the range of 35 – 50 V was chosen to study the dependence of the n_{eff} of the ATO films on the pore widening duration.
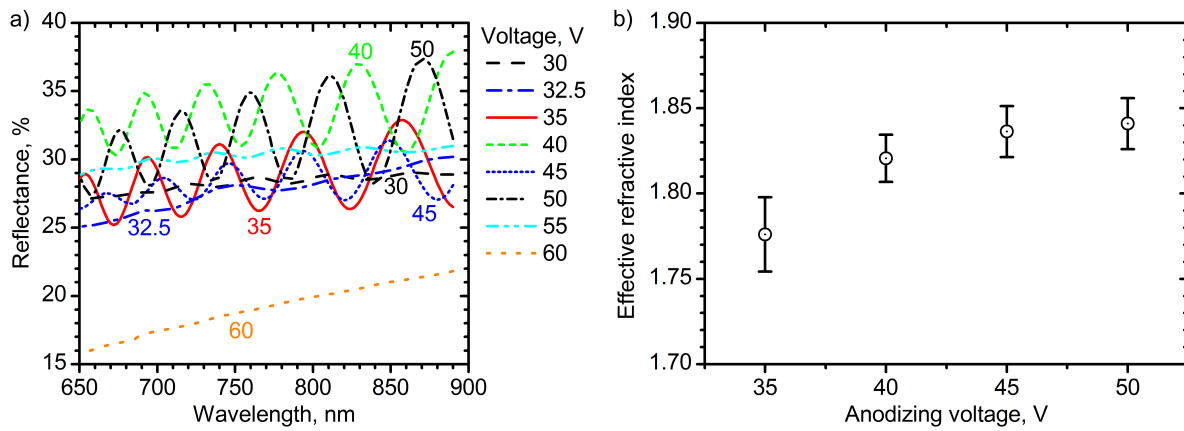

FIG. 1. Optical properties of ATO films prepared at various anodizing voltages. (a) Reflectance spectra recorded at incident angle of 8°. (b) The effective refractive index at 700 nm as a function of anodizing voltage

The positions of Fabry–Pérot oscillations in the spectra recorded at different incident angles were used for calculating the n_{eff} and sample thickness (h) using a protocol described previously [17]. The n_{eff} increases from 1.78 to 1.84 with growth of anodizing voltage from 35 to 50 V (Fig. 1b). Thickness-to-charge density ratio (h/q) lies in the range of 0.88 – 1.00 μm·cm^2·C^{-1}.

Typical SEM images of the ATO are shown in Fig. 2 on the example of the sample prepared at 35 V. ATO film consists of vertically aligned nanotubes contacting each other. The average distance between the centers of neighboring nanotubes (D_{int}) increases linearly from 79 to 111 nm with an increase in the anodizing voltage from 35 to 50 V; the proportionality constant D_{int}/U is 2.23 ± 0.03 nm V^{-1}, that is inside the range of corresponding value observed earlier for ethylene glycol based electrolytes (1.8 – 3.0) [14]. According to SEM data, the thickness of the samples prepared at $U = 35 – 50$ V is in the range of 2.9 – 3.2 μm, and thickness-to-charge density ratio lies in the range of 0.86 – 0.95 μm·cm^2·C^{-1}. It is worth noting that these values are in good agreement with spectral data.

The dependence of the effective refractive index of ATO films on the duration of chemical etching is shown in Fig. 3. Chemical etching of nanotube walls in F^{-}-containing electrolyte solution leads to the growth of the porosity of the ATO, resulting in a decrease in the n_{eff} (Fig. 3a). The rate of pore widening in electrolyte solution is slow enough: change of the n_{eff} after several hours of etching is lower than 0.11 independently of anodizing voltage. A stronger (up to 0.28) decrease in the n_{eff} is observed in the aqueous H_2O_2 solution (Fig. 3b). The rate of pore widening is substantially faster only during the first 15 minutes of etching. Further etching leads to a minor change in the n_{eff} followed by the detaching of ATO film after 30 min. Pore widening in H_2O_2 solution increases the difference between the n_{eff} of the layers obtained at 35 and 50 V (Δn_{eff}) from 0.06 to 0.14. The trend of the Δn_{eff} increase during pore widening is in good agreement with one reported for the anodic alumina films prepared in oxalic [18] and sulfuric acid electrolytes [16]. Most likely, the decrease in etching rate (decreasing of the n_{eff}) after 7.5 min in H_2O_2 is caused by layered structure of ATO pore walls. The inner layer, contacting with
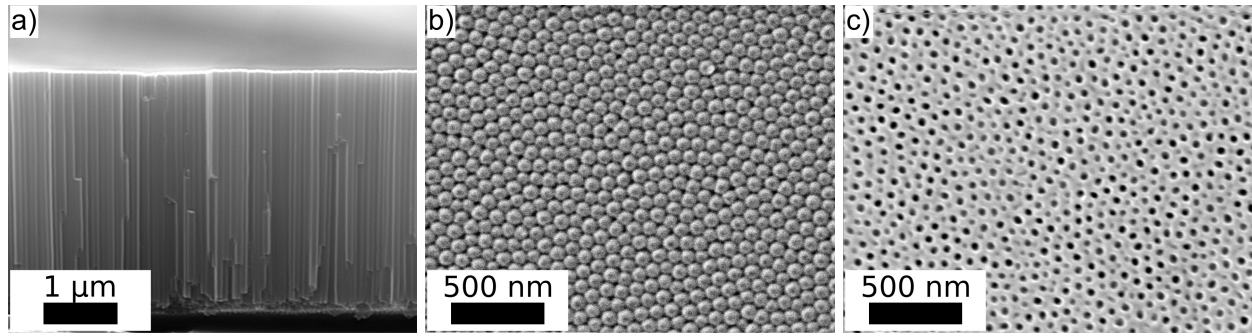
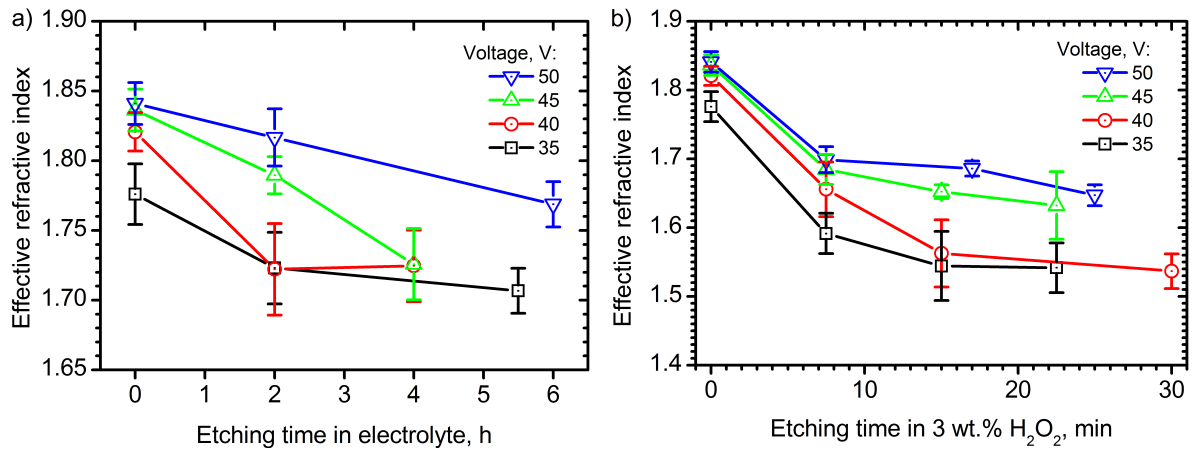FIG. 2. SEM images of the ATO film prepared at $U = 35$ V: cross section (a), bottom (b) and top view (c)

FIG. 3. Dependence of the effective refractive index at 700 nm on pore widening time for the ATO films prepared at 35 – 50 V: in the electrolyte (a) and in the 3 wt. % H_2O_2 aqueous solution (b)

electrolyte during anodizing, contains more impurities from electrolyte, that makes it less stable than the deeper layer consisting mainly of titania [19]. Obtained quantitative data on thickness and the n_{eff} of ATO will be in demand for the design of materials for antireflection coatings, memristive elements [20], photonic crystals [21], and solar cells.

4. Conclusions

High uniformity for the ATO film thickness was observed for the samples obtained in ethylene glycol electrolyte (0.3 wt. % NH_4F, 0.66 wt. % CH_3COONa, 2 wt. % H_2O) at anodizing voltages ranging from 35 to 50 V. The values of film thickness-to-charge density ratio vary from 0.86 to 1.00 $\mu m \cdot cm^2 \cdot C^{-1}$ according to analysis of the reflectance spectra and SEM images. The n_{eff} at 700 nm of the as-prepared ATO films is in the range of 1.78 – 1.84, which is higher than in the case of anodic alumina and bulk Al_2O_3. Pore widening in H_2O_2 solution allows one to achieve the lower bound of the n_{eff} of 1.54 and to increase the difference between the n_{eff} of the layers obtained at 35 and 50 V from 0.06 to 0.14. Chemical etching in aqueous H_2O_2 solution is an effective method for tuning the porosity of ATO films, saving their planarity and uniformity.

Acknowledgements

References

[1] Regonini D., Bowen C.R., Jaroenworaluck A., Stevens R. A review of growth mechanism, structure and crystallinity of anodized TiO_2 nanotubes. *Materials Science and Engineering: R: Reports*, 2013, **74** (12), P. 377–406.

[2] Shankar K., Mor G.K., et al. Highly-ordered TiO$_2$ nanotube arrays up to 220 μm in length: use in water photoelectrolysis and dye-sensitized solar cells. *Nanotechnology*, 2007, **18** (6), 065707.

[3] Varghese O.K., Paulose M., LaTempa T.J., Grimes C.A. High-rate solar photocatalytic conversion of CO$_2$ and water vapor to hydrocarbon fuels. *Nano Letters*, 2009, **9** (2), P. 731–737.

[4] Arfanis M.K., Adamou P., et al. Photocatalytic degradation of salicylic acid and caffeine emerging contaminants using titania nanotubes. *Chemical Engineering Journal*, 2017, **310**, P. 525–536.

[5] Varghese O.K., Gong D., et al. Hydrogen sensing using titania nanotubes. *Sensors and Actuators B: Chemical*, 2003, **93** (1), P. 338–344.

[6] Song Y.-Y., Schmidt-Stein F., Bauer S., Schmuki P. Amphiphilic TiO$_2$ nanotube arrays: an actively controllable drug delivery system. *Journal of the American Chemical Society*, 2009, **131** (12), P. 4230–4232.

[7] Gulati K., Kant K., Findlay D., Losic D. Periodically tailored titania nanotubes for enhanced drug loading and releasing performances. *Journal of Materials Chemistry B*, 2015, **3** (12), P. 2553–2559.

[8] Wang Q., Huang J.-Y., et al. Recent advances on smart TiO$_2$ nanotube platforms for sustainable drug delivery applications. *International Journal of Nanomedicine*, 2016, **12**, P. 151–165.

[9] Kim D., Ghicov A., Albu S.P., Schmuki P. Bamboo-type TiO$_2$ nanotubes: improved conversion efficiency in dye-sensitized solar cells. *Journal of the American Chemical Society*, 2008, **130** (49), P. 16454–16455.

[10] Wang G., Wang J., An Y., Wang C. Anodization fabrication of 3D TiO$_2$ photonic crystals and their application for chemical sensors. *Superlattices and Microstructures*, 2016, **100**, P. 290–295.

[11] Kim W.-T., Choi W.-Y. Fabrication of TiO$_2$ photonic crystal by anodic oxidation and their optical sensing properties. *Sensors and Actuators A: Physical*, 2017, **260**, P. 178–184.

[12] Zheng L., Cheng H., et al. Porous TiO$_2$ photonic band gap materials by anodization. *The Journal of Physical Chemistry C*, 2012, **116** (9), P. 5509–5515.

[13] DeVore J.R. Refractive indices of rutile and sphalerite. *JOSA*, 1951, **41** (6), P. 416–419.

[14] Cortes F.J.Q., Arias-Monje P.J., Phillips J., Zea H. Empirical kinetics for the growth of titania nanotube arrays by potentiostatic anodization in ethylene glycol. *Materials & Design*, 2016, **96**, P. 80–89.

[15] Sapoletova N.A., Kushnir S.E., Napolskii K.S. Anodic titanium oxide photonic crystals prepared by novel cyclic anodizing with voltage versus charge modulation. *Electrochemistry Communications*, 2018, **91**, P. 5–9.

[16] Kushnir S.E., Pchelyakova T.Yu., Napolskii K.S. Anodizing with voltage versus optical path length modulation: a new tool for the preparation of photonic structures. *Journal of Materials Chemistry C*, 2018, **6** (45), P. 12192–12199.

[17] Kushnir S.E., Napolskii K.S. Thickness-dependent iridescence of one-dimensional photonic crystals based on anodic alumina. *Materials & Design*, 2018, **144**, P. 140–150.

[18] Rahman M.M., Garcia-Caurel E., et al. Effect of the anodization voltage on the pore-widening rate of nanoporous anodic alumina. *Nanoscale Research Letters*, 2012, **7** (1), 474.

[19] Dronov A., Gavrilin I., et al. Investigation of anodic TiO$_2$ nanotube composition with high spatial resolution AES and ToF SIMS. *Applied Surface Science*, 2018, **434**, P. 148–154.

[20] Morozova P.A., Petukhov D.I. Preparation of Au/TiO$_2$/Ti memristive elements via anodic oxidation. *Nanosystems: Physics, Chemistry, Mathematics*, 2017, **8** (6), P. 823–829.

[21] Ermolaev G.A., Kushnir S.E., Sapoletova N.A., Napolskii K.S. Titania photonic crystals with precise photonic band gap position via anodizing with voltage versus optical path length modulation. *Nanomaterials*, 2019, **9** (4), P. 651.